J Mater Sci: Mater Med (2009) 20:329–337
DOI 10.1007/s10856-008-3590-3

Rapid biofabrication of tubular tissue constructs by centrifugal casting in a decellularized natural scaffold with laser-machined micropores

Vladimir A. Kasyanov · Jason Hodde · Michael C. Hiles · Carol Eisenberg · Leonard Eisenberg · Luis E. F. De Castro · Iveta Ozolanta · Modra Murovska · Robert A. Draughn · Glenn D. Prestwich · Roger R. Markwald · Vladimir Mironov

Received: 26 November 2007 / Accepted: 4 September 2008 / Published online: 20 September 2008

Abstract Centrifugal casting allows rapid biofabrication of tubular tissue constructs by suspending living cells in an in situ cross-linkable hydrogel. We hypothesize that introduction of laser-machined micropores into a decellularized natural scaffold will facilitate cell seeding by centrifugal casting and increase hydrogel retention, without compromising the biomechanical properties of the scaffold. Micropores with diameters of 50, 100, and 200 μm were machined at different linear densities in decellularized small intestine submucosa (SIS) planar sheets and tubular SIS scaffolds using an argon laser. The ultimate stress and ultimate strain values for SIS sheets with laser-machined micropores with diameter 50 μm and distance between holes as low as 714 μm were not significantly different from unmachined control SIS specimens. Centrifugal casting of GFP-labeled cells suspended in an in situ cross-linkable hyaluronan-based hydrogel resulted in scaffold recellularization with a high density of viable cells inside the laser-machined micropores. Perfusion tests demonstrated the retention of the cells encapsulated within the HA hydrogel in the microholes. Thus, an SIS scaffold with appropriately sized microholes can be loaded with hydrogel encapsulated cells by centrifugal casting to give a mechanically robust construct that retains the cell-seeded hydrogel, permitting rapid biofabrication of tubular tissue construct in a "bioreactor-free" fashion.

V. A. Kasyanov · C. Eisenberg · L. Eisenberg · L. E. F. De Castro · R. A. Draughn · R. R. Markwald · V. Mironov (✉)
Medical University of South Carolina, Charleston, SC 29426, USA
e-mail: mironovv@musc.edu

V. A. Kasyanov · I. Ozolanta · M. Murovska
Riga Stradins University, Riga 1007, Latvia

J. Hodde · M. C. Hiles
Cook Biotech Inc, West Lafayette, IN 47906, USA

G. D. Prestwich
Department of Medicinal Chemistry, Center for Therapeutic Biomaterials, The University of Utah, Salt Lake City, UT 84108-1257, USA

1 Introduction

Small diameter tissue-engineered vascular grafts are considered a holy grail for vascular surgery [1, 2]. During the past two decades, great progress has been made in using decellularized extracellular scaffolds [3–6] for vascular tissue engineering [7–9]. Among these, the acellular small intestine submucosa (SIS) has been suggested as a vascular prostheses and a scaffold for tissue-engineered vascular graft [10–12]. In canine models, the acellular vascular graft remains patent for up to 5 years [13]. However, endogenous endothelization is variable in different experimental animal models, and it is thought that in humans the effective, spontaneous in vivo endothelization of acellular scaffold would not occur without a targeting mechanism to attract cells. Thus, xenogenic porcine SIS must be endothelialized in order to reduce thrombogenicity and improve graft biocompatibility. While SIS can be endothelialized in vitro [10, 14], endothelization with autologous patient-derived cells would be problematic. Such a therapy would only be appropriate for patients with planned surgery, because recellularization of cardiovascular implants with host cells prior to implantation is not an intraoperative procedure; several weeks advance planning would be required.

Rapid transmural capillary ingrowth provides a source of intimal endothelium and smooth muscle in porous PTFE prostheses [15]. Any modifications of vascular graft processing which can enhance in vivo recellularization will improve clinical utility. For example, laser perforation of chemically stabilized natural acellular vascular graft materials [16, 17] has been explored as a potential mechanism for improving post-implantation endothelization and remodeling. Thus, spontaneous endothelization of biosynthetic ovine vascular prostheses (Omniflow, Bionova, Melbourne, Australia) can be achieved by transmural capillary ingrowth through laser-made perforations in the wall of prostheses in an experimental sheep model [17]. In vivo endothelization of vascular matrix through laser-made micropores (ovine carotid arteries decellularized by dye-mediated photooxidation Photofix TM, Sulzer-Carbomedics, Austin, TX, USA) [16] have been also demonstrated. However, 6 months after implantation, thicker and more differentiated intima had formed in the laser-perforated graft. The authors concluded that enhanced endothelial coverage did not improve graft patency because inadequately controlled intimal thickening overshadowed the expected benefit of enhanced endothelization [16, 17]. In other studies, in vivo cell seeding of expanded polytetrafluoroethylene graft with immobilized anti-CD34 antibodies successfully accelerated endothelization but also stimulated intimal hyperplasia [18]. Thus, in vivo endothelial progenitor cell-seeded grafts could be potentially risky [19, 20]. Based on these observations it appears that (i) micropore size and density, (ii) the mechanical properties of scaffold (mechanical compliance), and (iii) the biological characteristics (activation, quiescence and level of differentiation and plasticity) of recruited endothelial progenitor cells or endothelial cells are all important determinants of the long-term patency of vascular grafts based on laser-perforated acellular scaffolds.

We recently developed centrifugal casting technology [21] which allows rapid recellularization of a tubular vascular scaffold cells suspended within an in situ cross-linkable hyaluronan hydrogel [22]. Additional preliminary experiments then demonstrated that retention of such a hydrogel on an acellular vascular scaffold was very poor, most likely due to weak adhesion between the hydrogel and inner wall of the scaffold. We hypothesized that using laser perforation would create a microporous scaffold which could undergo more rapid recellularization and show increased hydrogel retention without compromising biomechanical properties of the scaffold. Moreover, the laser-perforated scaffold combined with a centrifugally cast biomimetic functional hydrogel containing embedded cells could both enhance the desired endothelization while preventing the undesired intimal thickening in vivo.

Development of rapid biofabrication technology which ensures retention of hydrogel and cell viability in porous scaffold and does not alter biomechanical properties of hydrogel is the first critically important step in this approach. Herein we report that laser-machining of micropores of optimal size and density in a decellularized natural SIS scaffold, in combination with centrifugal casting of in situ cross-linkable hydrogel, does not compromise biomechanical properties of scaffold. Moreover, the resulting construct shows improved retention of hydrogel and the encapsulated cells, and paves the way for development of a rapid "bioreactor-free" biofabrication of tubular tissue-engineered constructs.

2 Materials and methods

2.1 Material

To investigate the influence of diameter of laser-machined micropores and distance between them on the mechanical properties of a scaffold (Fig. 1), small intestinal submucosa (SIS) plane sheets (Cook Biotech Inc., West Lafayette, IN) [4] were used as experimental material. The wall thickness of SIS plane sheets was 0.152 ± 0.012 mm.

The SIS plane sheet samples were divided into four groups:

(1) Specimens with micropores of diameter 50 μm (5 sheets with 3 micropores, 5 sheets with 6 micropores and 5 sheets with 9 micropores along the 5 mm width);
(2) Specimens with micropores of diameter 100 μm (5 sheets each having 3, 6, or 9 micropores as above);

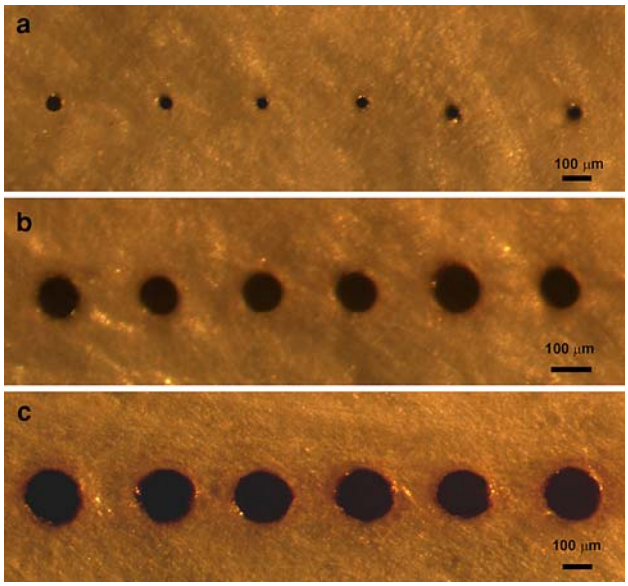

Fig. 1 Scheme of laser-machined micropores: (**a**) diameter 50 μm, (**b**) 100 μm and (**c**) 200 μm

(3) Specimens with micropores of diameter of 200 μm (5 sheets each having 3, 6, or 9 micropores as above);
(4) Control non-perforated SIS specimens (5 specimens, no micropores).

Five laser-perforated tubular SIS scaffolds of diameter 5 mm were used for centrifugal casting cell seeding and for sequential hydrogel retention test.

2.2 Laser machining of micropores

The SIS samples were placed in front of the slit lamp of an argon laser delivery system (488 nm and 519 nm, model Novus 2000; Coherent, Inc., Santa Clara, CA). Individual burns were produced using focused laser spots at the marked sites of the specimens with a beam diameter of 50 μm for 0.5 s of duration at 900 mW, a beam diameter 100 μm for 0.5 s at 830 mW, and a beam diameter of 200 μm for 0.2 s at 700 mW. Laser applications were placed one spot size apart and the treatment goal was to keep the burns as light as possible. To make micropores in SIS tubular scaffold the scaffold was mounted on a glass rod which was inserted into a positioning device. The micropores of diameter 50 μm were burned using a template that maintained a distance of 0.75 mm between the scaffold and the laser.

2.3 Tensile tests

Dumb-bell shaped samples 5.0 mm wide in the middle zone ($n = 50$) were cut with a template in order to perform tensile tests. Tensile tests were performed using an MTS tensile test system (The 858 Mini Bionix II Test System). Force-elongation curves were recorded at an elongation rate of 5 mm min^{-1} [23] (this elongation rate usually is used for quasi-static tensile test of soft biological tissue and biomaterials) until a rupture of specimen, and then ultimate stress and ultimate strain were calculated.

2.4 Cell culture

Mesodermal quail QCE-6 cells [24] transfected with green fluorescent gene (GFP) were grown in medium consisting of media M199 (Fisher) supplemented with 10% chicken serum (Fisher) 100 U/ml penicillin, and 100 μg/ml streptomycin sulfate. All cells were incubated in a humidified 37°C 5% CO_2 environment with growth media replaced every 3–4 days. The cells were expanded to 80–90% confluence prior to trypsinization for passage or centrifugal casting.

2.5 Preparation and cell seeding of the sECM

Thiolated HA and thiolated gelatin and were dissolved in media 199 to give 1.25% (w/v) and 3.0% (w/v) solutions, respectively, and the solution pH was adjusted to 7.4 by adding 0.1 m NaOH solution [22]. Polyethylene glycol diacrylate (PEGDA Mw 3400, Nektar) was also dissolved in media 199 to give a 4.5% (w/v) solution. All the above solutions were then sterilized by filtering through 0.45 μm filter. Next, a solution of thiolated HA and thiolated gelatin was prepared by mixing 2.8 ml thiolated HA solution and 1.2 ml thiolated gelatin solution. The pellet of centrifuged cells was then very gently mixed to suspend the cells in the with the HA/gelatin solution (volume of cells: volume of solution = 1:3); immediately after adding cells, the PEGDA solution was added to cell suspension in a volume ratio of 1:4 to initiate the crosslinking and gelation. Thus cells occupied approximately 20% of volume of gel/cell mixture. After careful mixing, the final cell suspension in the gelling solution was placed in glass tubes for centrifugal casting.

2.6 Centrifugal casting

Centrifugal casting of perforated and non-perforated SIS scaffolds with in situ cross-linkable hydrogel was performed as previously described (Fig. 2) [21].

Shortly before fabrication, the volume of hydrogel layer and cells was calculated on the basis of given thickness of the layer (0.2 mm) and length of the tube (less the length of stoppers in the tube). Pyrex glass tubes B-YF-WG6 (Small Parts Inc.) with inner diameter 5.0 ± 0.1 mm were used for spinning. Tubes were 45 ± 0.2 mm in length, and the ends were closed using translucent Fisher brand solid silicon stoppers. The SIS scaffold was placed in the glass tube, and the estimated volume of the suspension of in situ cross-linkable hydrogel and living QCE-6 cells was placed in the SIS scaffold. The glass tube was tightly closed with silicon stoppers and then fixed in the spinner. The glass tube was spun with a speed of 2,000 rpm for 10 min, during which time the hydrogel cross-linked.

2.7 Hydrogel retention and scaffold permeability test

The hydrogel retention test was performed in the perfusion bioreactor [25, 26] with M199 media at 37°C. After

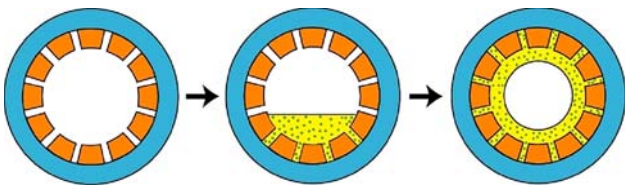

Fig. 2 Images of centrifugal casting of laser-perforated tubular SIS scaffold with in situ cross-linkable hyaluronan-based hydrogel and living cells

centrifugal casting, the tubular SIS scaffold was placed in the chamber of bioreactor and was perfused under an internal pressure of 100 mmHg. A steady flow rate of media inside the SIS scaffold was maintained at 500 ml/min during 30 min. The hydrogel retention test was considered negative if, after performing perfusion at physiological level of hydrodynamics, all perforations under microscopy observation contained living GFP-labeled cells embedded in polymerized hydrogel and no open (cell free) pores were observed.

The water permeability of the SIS scaffold with laser-machined micropores of diameter 50 μm was tested after centrifugal casting with hydrogel and cells using a perfusion bioreactor [21]. The scaffold was placed in a chamber and was cannulated and tied at both ends. The scaffolds were loaded by internal pressure at 120, 180, 200 and 220 mmHg while maintaining the length of the sample constant. The standard procedure of water permeability determination was used as described in [27]. The pressure was held constant at each step for 1 min and volume of water passing through the wall under each fixed hydrostatic pressure was collected.

2.8 Cell viability test

Due to technological difficulties of sectioning of hyaluronan hydrogel, the GFP-labeled cells have been employed for the study of cell viability in centrifugally cast specimens without histological processing. As shown previously [21], cell death is associated with loss of GFP fluorescence. The percentage of GFP-positive and GFP-negative cells used or embedded in the in situ cross-linkable hydrogel were estimated before and after centrifugal casting, respectively.

2.9 Microscopy

Laser-perforated tubular SIS scaffolds seeded with living cells by centrifugal casting were analyzed in non-fixed conditions under phase/fluorescent microscope (Nikon TE2000S, Japan).

2.10 Statistics

The ultimate stress and ultimate strain were expressed as mean values plus one standard deviation. A total of 50 specimens were analyzed. Groups of data were analyzed by single-factor ANOVA. A P value of less than 0.05 was considered statistically significant. When only two groups were being compared, data were analyzed using Student's t-tests with a P value of less than 0.05 indicating statistical significance.

3 Results

3.1 Mechanical properties of laser-perforated SIS samples

Experimental results of tensile tests of samples with different quantities of laser-machined micropores showed that for micropores with a diameter of 50 μm, there was no statistical difference ($P > 0.05$) between ultimate stress for control non-perforated samples and samples with either three or six micropores: 57.09 ± 2.27 MPa, 56.63 ± 3.13 MPa and 52.83 ± 2.95 MPa, respectively (Fig. 3a). This suggests that a distance of 714 μm or greater between the holes (i.e., six holes per 5 mm length) does not significantly decrease the ultimate stress. In contrast, the ultimate stress of samples which have nine laser-machined micropores per 5 mm length was less ($P < 0.05$) than the ultimate stress of unperforated samples (57.09 ± 2.27 MPa vs. 47.10 ± 5.93 MPa, respectively).

Increasing the diameter of the micropores to 100 μm leads to a significant decrease in ultimate stress of samples (Fig. 3b). For example, at three micropores per 5-mm width, the ultimate stress decreases to 53.8% in comparison with ultimate stress for unperforated specimens. With six micropores of 200 μm diameter, the ultimate stress decreased threefold times relative to controls (16.77 ± 1.39 MPa vs. 57.09 ± 2.27 MPa, respectively).

The ultimate strain (Fig. 3c) of SIS specimens with six 50-μm micropores did not differ statistically ($P > 0.05$) from that for non-perforated SIS specimens (8.8 ± 0.87% and 9.8 ± 0.53%, respectively). However, 100- and 200-μm micropores significantly decreased the ultimate strain of specimens to 2.94 ± 0.66% and 2.36 ± 0.45%, respectively. These values are statistically different from the ultimate strain of non-perforated specimens ($P < 0.05$). Thus, the experimental results show that laser-machined micropores of diameter 50 μm do not compromise the mechanical properties of SIS material if the distance between micropores does not exceed 714 μm.

3.2 Centrifugal casting of tubular tissue constructs

Microscopic analysis of laser-perforated tubular scaffolds after centrifugal casting demonstrated that every micropore contained GFP-positive viable cells at high cell density (Fig. 4). Although occasional cells can be observed on the inner surface of the tubular scaffold, most of the cells were located inside the hydrogel-filled micropores.

3.3 Cell viability

The number of GFP positive cells in the in situ cross-linkable hydrogel were not significantly different before or after

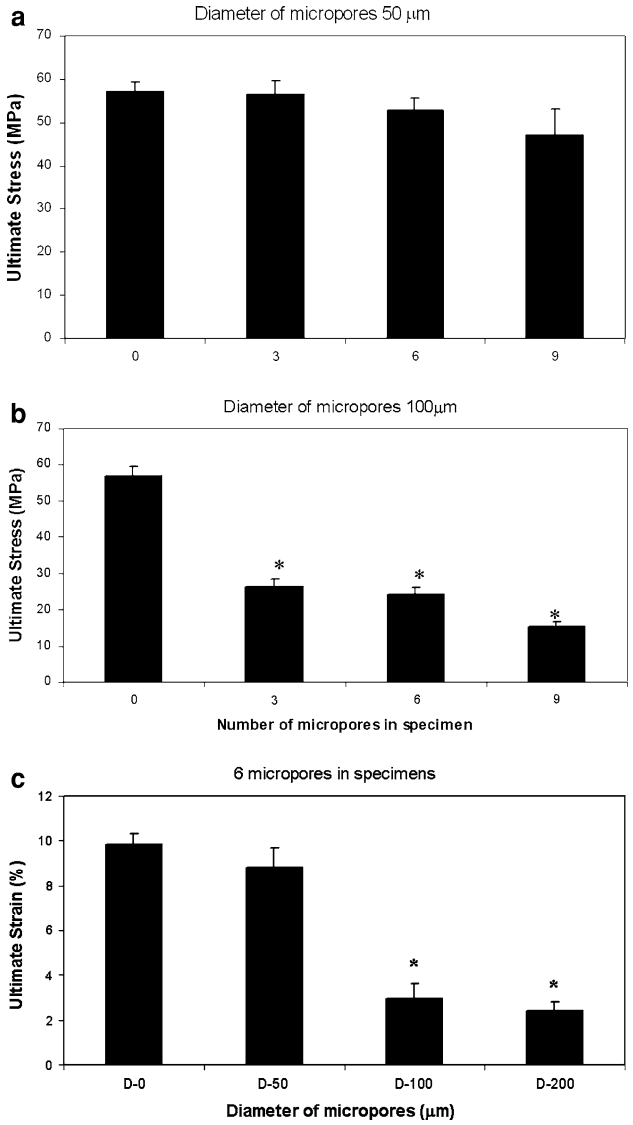

Fig. 3 (**a**) Ultimate stress for whole SIS specimens and specimens with laser-machined micropores (3, 6 and 9 micropores of diameter 50 μm). Statistical significance is denoted by asterisks. (**b**) Ultimate stress for whole SIS specimens and specimens with laser-machined micropores (3, 6 and 9 micropores of diameter 100 μm). Statistical significance is denoted by asterisks. (**c**) Ultimate strain for whole SIS specimens and specimens with different diameter of laser-machined micropores (50, 100 and 200 μm) at six micropores along the width of specimen. Statistical significance is denoted by asterisks

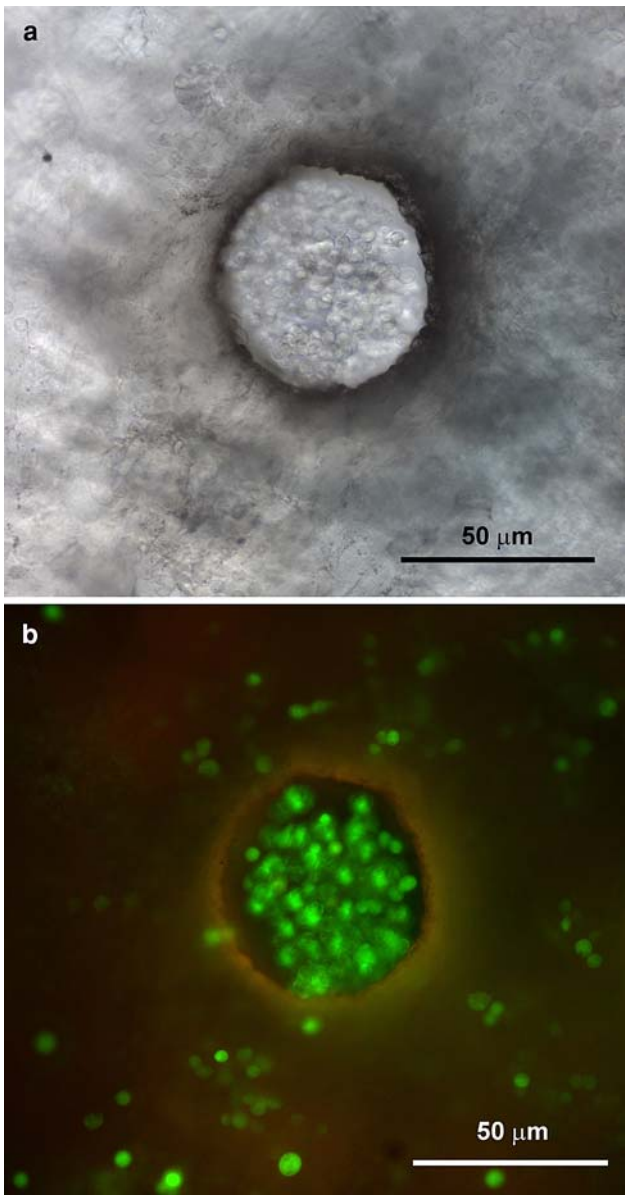

Fig. 4 Laser-machined micropores before and after cell seeding by centrifugally casting using in situ cross-linkable hydrogel. (**a**) Phase contrast microscopy of densely packed QCE-6 mesodermal cells in laser-machined micropores after centrifugal casting of perforated decellularized SIS scaffolds. (**b**) Fluorescent microscopy of GFP-labeled QCE-6 mesodermal cells in laser-machined micropores after centrifugal casting of perforated decellularized SIS scaffolds. Green staining indicates cells viability. Rare, randomly redistributed cells are seen on the internal surface of SIS scaffold

centrifugal casting (Fig. 5). Additional controlled experiments demonstrated that neither the addition of the cross-linking mixture without centrifugation, the centrifugation process, nor the hydrogel cross-linking chemistry, resulted in any statistical difference with respect to cell viability (data not shown).

3.4 Hydrogel retention and permeability test

The hydrogel retention of the SIS scaffold with laser-machined micropores was estimated microscopically after centrifugal casting by determining the presence of cells in hydrogel-filled micropores. From the collected volumes of water during each of the 1 min of testing, average values of water permeability of scaffold ($n = 3$) were calculated. The water permeability was not determined at 120 and 180 mmHg, there were not leaks, drops and wettening of perfused scaffold. No signs of hydrogel loss or associated

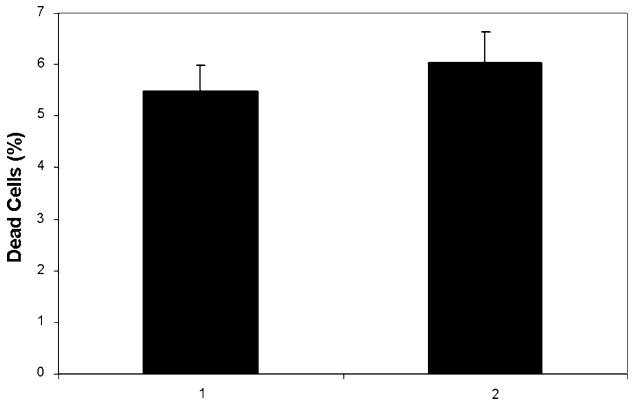

Fig. 5 Effect of centrifugal casting on viability of QCE-6 cells. 1—Percent of dead QCE-6 in hydrogel suspension before centrifugal casting. 2—Percent of dead QCE-6 cells in polymerized hydrogel after centrifugal casting. There is no statistic difference ($P > 0.05$)

leakage through the scaffold wall were observed at these inner pressures. The data show that water permeability at inner pressure 200 mmHg was 1.06 ± 0.22 ml/min/cm^2, and at 220 mmHg was 1.68 ± 0.34 ml/min/cm^2, respectively.

4 Discussion

The main goal of this study was to demonstrate the feasibility of rapid biofabrication of a tissue-engineered vascular construct using centrifugal casting technology in combination with a laser-perforated natural scaffold. Centrifugal casting allows rapid formation of cellularized cylindrical constructs by permitting gelation of a suspension of living cells in an in situ cross-linkable hydrogel during axial centrifugation [21]. In preliminary experiments with an acellular natural scaffold, we observed poor retention of hydrogel on the scaffold. This appeared to be the result of the low adhesivitiy of the hydrogel to the inner surface of the scaffold. We hypothesized that the laser-machining of micropores in the decellularized natural scaffold would improve hydrogel retention and thereby enable cell seeding by centrifugal casting, with cells being encapsulated in the hydrogel that would be entrapped within the pores. First, we needed to establish a pore size and pore density that would not compromise the biomechanical properties of the scaffold. We selected SIS as a model system. SIS is a well investigated and characterized decellularized natural scaffold [4], which has also been used as a vascular graft [11, 28–30].

To determine the optimal diameter and density of laser-machined micropores, SIS sheets were patterned with three different micropore diameters (50, 100, and 200 μm) at three linear densities (3, 6, and 9 pores per 5 mm). We sought to determine the optimal micropore density which would (i) provide enough space for effective recellularization using centrifugal casting, (ii) allow sufficient hydrogel retention, and (iii) maintain the biomechanical properties of the scaffold. We found that the ultimate stress and ultimate strain of SIS sheets with laser-machined micropores with diameter 50 μm and distance between holes of at least 714 μm did not differ statistically from unperforated control SIS sheets. Based on these data we proposed an optimal pattern of micropore size, density and redistribution (Fig. 6). Our data are consistent with the diameter of micropores suggested for increasing post-implantation in vivo endothelization of natural scaffolds as described by the group that pioneered laser perforation of natural scaffolds [16, 17]. Laser perforation was first used to machine micropores of 50–100 μm in diameter separated by 4 mm [17], and then employed to make 50 μm pores at a density of 50 holes/cm^2 [16]. In both cases, laser perforation was reported to enhance post-implantation endothelization of employed two variants of vascular grafts (Omniflow—BioNova, Australia and Sultzer-Carbomedics, Austin, Texas) [16, 17]. Similarly, synthetic vascular graft pores ranging in diameter from 30–60 μm enhanced in vivo endothelization of synthetic porous vascular graft through transmural vascularization [15]. It is likely that the optimal diameter and density determined in this study will also enable transmural vascularization and enhance post-implantation endothelization without compromising biomechanical properties of vascular graft.

The hydrogel selected was a semi-synthetic extracellular matrix (sECM) equivalent that was developed for cell therapy, reparative medicine, toxicology models, bioprinting [31] and 3-D cell culture [32, 33]. The sECM hydrogel

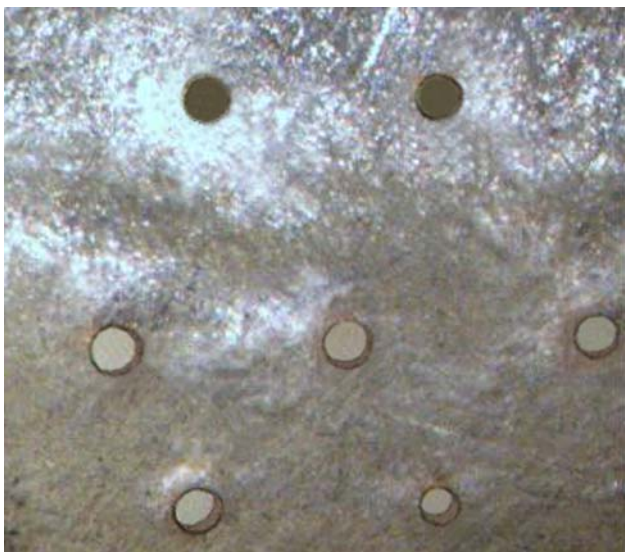

Fig. 6 Decellularized SIS tubular scaffold with biomechanically optimal hexagonal pattern of laser-machined micropores

is composed of chemically modified hyaluronan and gelatin components that can be readily cross-linked in 5–30 min with cytocompatible crosslinkers [34]. It has been employed for delivery of autologous mesenchymal stem cells for osteochondral defect repair in rabbits [35], for in vivo liver repair in mice using rat and human hepatocytes [32], and for growth of mature adipose tissue from human adipose-derived stem cells [36]. This sECM meets the important translational constraints that the material should be approvable for use in humans, simple, manufacturable, and easy to use [32]. In addition, these sECMs can be loaded with angiogenic growth factors that dramatically accelerate angiogenesis and the formation of mature microvasculature in vivo [37–39]. Importantly, growth-factor loaded hydrogels are able to accelerate wound healing and create a vascularized neodermis in a diabetic mouse model for chronic, non-healing wounds [40].

There are several significant differences between the approach described herein and previous laser-perforated scaffold systems. First, the Austrian group [16, 17] did not use centrifugal casting combined with an in situ cross-linkable hydrogel. The extracellular matrix for transmural angiogenesis was provided in vivo by deposition of fibrin from perfused blood as result of microthromboses associated with the micropores. Second, the micropores in the previous vascular graft were not seeded with exogenous living cells, and thus recellularization was able to be accomplished in vivo. Third, we employed a non cross-linked acellular natural matrix which could be a subject of post-implantation in vivo remodeling, rather than a cross-linked decellularized matrix. Basically, rather than make an incremental improvement, we sought to develop a novel tissue engineering technology for rapid biofabrication of cellularized vascular tissue constructs.

To test the ability of the laser-perforated scaffold to retain a hydrogel sECM containing encapsulated cells, we used GFP positive mesodermal cells from an avian source. We selected the scaffolds with 50 μm micropores, since these did not compromise the strength of the scaffold. We found that these pores were effectively and rapidly recellularized with living cells following 10 min of centrifugal casting. As reported previously, centrifugally cast cell-hydrogel suspensions result in a very high level of viability, indicating neither the centrifugal forces (ca. $11 \times g$) nor the in situ cross-linking process causes chemical or physical damage to the encapsulated cells [21]. Moreover, centrifugal casting also provided the desired cell density within the micropores, a parameter that can be further adjusted by simply changing the cell concentration in the pre-gelled suspension. Additionally, as shown by the perfusion retention test, the laser-perforated scaffolds provided much improved hydrogel retention in the scaffold. At a physiological blood pressure, no undesirable pressure-induced leaks were visually observed. Finally, the cell seeding using centrifugal casting was achieved in only 10 min, without the use of a perfusion bioreactor. This feature substantially reduces the time and expense for preparing a cellularized construct. Taken together, centrifugal casting in combination with a laser-perforated "off-the-shelf" acellular scaffold and an sECM in situ cross-linkable hydrogel designed for cell therapy applications offers a rapid, "bioreactor-free" method for cell seeding.

Importantly, centrifugal casting of laser-perforated biomechanically robust acellular natural scaffolds could be used for rapid biofabrication of variety of both tubular and planar (folded into tube) tissue-engineered constructs. A variety of natural allogeneic and xenogeneic acellular scaffolds are already approved for human use [3].

Does the hyaluronan-based sECM hydrogel improve the retention and proliferation of the encapsulated cells, and can it contribute to cellular differentiation and remodeling to form an implantable tissue-engineered vascular replacement? Could this be used intraoperatively with autologous cells, or is this an unnecessary additional procedure without any potential benefit? In order to address this question, we must consider potential negative outcomes and complications that can occur after implantation of laser-perforated vascular graft.

Six months after implantation, laser-perforated acellular vascular grafts develop intimal thickening that is almost twice that observed in non-perforated control grafts [16]. It appears that endothelization of the perforated materials may actually promote intimal thickening. This paradoxical result has been previously reported. For example, Conte et al. [41] demonstrated that graft endothelization increased intimal thickening. Moreover, in vivo cell seeding of an expanded polytetrafluoroethylene with immobilized anti-CD34 antibodies successfully accelerates endothelization but also stimulates intimal hyperplasia [18]. Thus, in vivo endothelial progenitor cell-seeded grafts could be potentially risky [19]. Kaushal et al. [9] demonstrated that seeding of acellular scaffolds in bioreactors perfused by bone marrow derived endothelial progenitor cells can lead to formation both endothelial and smooth muscle cells. Rapid vascular graft endothelization using the "sodding technique" also leads to development of intimal thickening [42].

Taken together, these data strongly suggest that endothelization (at least in certain situations) could promote undesired intimal thickening. There are at least two potential cellular mechanisms that can explain development of endothelization associated intimal thickening: (i) endothelial-mesenchymal transformation [43], and (ii) recruitment of circulating progenitor cells by activated endothelium followed by their differentiation into collagen-producing cells [44]. Both activated endothelial cells and endothelial progenitor cells with insufficient levels of

differentiation, quiescence and confluence can contribute to this outcome. These cells have the potential to either enhance recruitment of circulated endothelial progenitor cells, or to undergo differentiation and transdifferentiation into myofibroblast-like alpha-smooth muscle actin positive collagen-producing intimal cells [45]. One strategy to minimize intimal thickening would be to reduce cell adhesion to the substratum through the use of a cell-free in situ cross-linkable athrombogenic hydrogel. Indeed, hyaluronan-based hydrogels are broadly used for non-thrombogenic coating medical device and catheters [26]. Moreover, the in situ cross-linkable hyaluronan gels analogous to the sECM used herein has low cell adhesivity and has been employed for prevention of post-surgical adhesions in abdominal surgeries [46].

A second strategy employs the in situ cross-linkable sECM hydrogel modified in such way that it can potentially enhance desirable endothelization while simultaneously preventing undesirable intimal thickening in vivo. The in situ cross-linkable hydrogel can be augmented with angiogenic and endotheliogenic factors (e.g., angiopoetin-1, vascular endothelial growth factor, basic fibroblast growth factor) using the sECM technology [38, 39, 47]. The delivery of single or dual growth factors from an sECM promotes in vivo post-implantation angiogenesis [37, 38] and associated transmural angiogenesis induced endothelization. These constructs are also efficient in accelerating closure, remodeling, and revascularization of wounds in diabetic animals [40]. More cell-specific recruitment of circulating endothelial progenitor cells with concomitant rapid formation of confluent quiescent endothelial monolayers can be achieved with sECM hydrogels incorporating functional peptides [48–50] or specific antibodies. The hydrogel-mediated directed differentiation of encapsulated cells into desired cell lineages or directed modification of cell and tissue phenotypes is a reasonable outcome using this strategy.

Finally, it is important to indicate that the presence of living cells in laser-perforated centrifugal cast scaffolds with estimated micropore distance of 714 μm is permissive for effective post-implantation recellularization of acellular matrix. The use of in situ cross-linkable sECM hydrogels with well defined and tailored chemical functionalities would enable these studies. Testing a laser-perforated, biomechanically compliant, acellular natural tubular scaffold containing centrifugally cast cells in an sECM in vivo will be pursued in due course.

5 Conclusion

We have shown that laser-machined micropores of an optimal size and density in a decellularized natural SIS scaffold can be combined with centrifugal casting of a cell-seeded, in situ cross-linkable hydrogel. The laser perforation does not compromise biomechanical properties of scaffold, and substantially improves the hydrogel and cellular retention by the scaffold. This rapid, "bioreactor-free" biofabrication of tubular tissue-engineered construct has the potential for using cost-effective, "off-the-shelf" materials to create implantable tissue-engineered vascular grafts. Moreover, the constructs will allow systematic studies in vivo to probe the molecular and cellular mechanisms of endothelization and vascular intimal thickening. The constructs can also explore permissive and non-permissive conditions for recruitment of circulated endothelial progenitor and stem cells and acellular scaffold recellularization and remodeling.

Acknowledgments This research was supported by NSF FIBR Grant (EF-0526854). GDP also thanks the NIH (DC004336) and the Utah Centers of Excellence Program for financial support.

References

1. M.S. Conte, FASEB J. **12**, 43 (1998)
2. J.D. Kakisis, C.D. Liapis, C. Breuer, B.E. Sumpio, J. Vasc. Surg. **41**, 349 (2005)
3. S.L. Dahl, J. Koh, V. Prabhakar, L.E. Niklason, Cell Transplant. **12**, 659 (2003)
4. J. Hodde, Tissue Eng. **8**, 295 (2002)
5. Q. Lu, K. Ganesan, D.T. Simionescu, N.R. Vyavahare, Biomaterials **25**, 5227 (2004)
6. C.E. Schmidt, J.M. Baier, Biomaterials **21**, 2215 (2000)
7. G.E. Amiel, M. Komura, O. Shapira, J.J. Yoo, S. Yazdani, J. Berry, S. Kaushal, J. Bischoff, A. Atala, S. Soker, Tissue Eng. **12**, 2355 (2006)
8. T. Huynh, G. Abraham, J. Murray, K. Brockbank, P.O. Hagen, S. Sullivan, Nat. Biotechnol. **17**, 1083 (1999)
9. S. Kaushal, G.E. Amiel, K.J. Guleserian, O.M. Shapira, T. Perry, F.W. Sutherland, E. Rabkin, A.M. Moran, F.J. Schoen, A. Atala, S. Soker, J. Bischoff, J.E. Mayer Jr, Nat. Med. **7**, 1035 (2001)
10. S. Badylak, A. Liang, R. Record, R. Tullius, J. Hodde, Biomaterials **20**, 2257 (1999)
11. G.C. Lantz, S.F. Badylak, M.C. Hiles, A.C. Coffey, L.A. Geddes, K. Kokini, G.E. Sandusky, R.J. Morff, J. Invest. Surg. **6**, 297 (1993)
12. G.J. Wilson, D.W. Courtman, P. Klement, J.M. Lee, H. Yeger, Ann. Thorac. Surg. **60**, S353 (1995)
13. G.J. Wilson, H. Yeger, P. Klement, J.M. Lee, D.W. Courtman, ASAIO Trans. **36**, M340 (1990)
14. O.E. Teebken, A. Bader, G. Steinhoff, A. Haverich, Eur. J. Vasc. Endovasc. Surg. **19**, 381 (2000)
15. A.W. Clowes, T.R. Kirkman, M.A. Reidy, Am. J. Pathol. **123**, 220 (1986)
16. H. Bergmeister, P. Boeck, M.T. Kasimir, T. Fleck, F. Fitzal, W. Husinsky, M. Mittlboeck, H.G. Stoehr, U. Losert, E. Wolner, M. Grabenwoeger, J. Biomed. Mater. Res. B. Appl. Biomater. **74**, 495 (2005)
17. M. Grabenwoger, F. Fitzal, J. Sider, C. Cseko, H. Bergmeister, H. Schima, W. Husinsky, P. Bock, E. Wolner, Ann. Thorac. Surg. **66**, S110 (1998)
18. J.I. Rotmans, J.M. Heyligers, H.J. Verhagen, E. Velema, M.M. Nagtegaal, D.P. De Kleijn, F.G. De Groot, E.S. Stroes, G. Pasterkamp, Circulation **112**, 12 (2005)

19. J.I. Rotmans, J.M. Heyligers, E.S. Stroes, G. Pasterkamp, Can. J. Cardiol. **22**, 1113 (2006)
20. P. Roy-Chaudhury, Circulation **112**, 3 (2005)
21. V. Mironov, V. Kasyanov, X. Zheng Shu, C. Eisenberg, L. Eisenberg, S. Gonda, T. Trusk, R.R. Markwald, G.D. Prestwich, Biomaterials **26**, 7628 (2005)
22. X.Z. Shu, Y. Liu, Y. Luo, M.C. Roberts, G.D. Prestwich, Biomacromolecules **3**, 1304 (2002)
23. Sharma MG (1976) J Biomech 293
24. C.A. Eisenberg, R.R. Markwald, Dev. Biol. **191**, 167 (1997)
25. V. Mironov, V. Kasyanov, K. Mcallister, S. Oliver, J. Sistino, R. Markwald, J. Craniofac. Surg. **14**, 340 (2003)
26. V. Mironov, V.A. Kasyanov, M.J. Yost, R. Visconti, W. Twal, T. Trusk, X. Wen, I. Ozolanta, A. Kadishs, G.D. Prestwich, L. Terracio, R.R. Markwald, J. Long Term Eff. Med. Implants **16**, 111 (2006)
27. M.W. King, R.G. Guidoin, K.R. Gunasekera, C. Gosselin, Med. Prog. Technol. **9**, 217 (1983)
28. S.T. Herbert, S.F. Badylak, L.A. Geddes, B. Hillberry, G.C. Lantz, K. Kokini, Ann. Biomed. Eng. **21**, 727 (1993)
29. M.C. Hiles, S.F. Badylak, L.A. Geddes, K. Kokini, R.J. Morff, J. Biomed. Mater. Res. **27**, 139 (1993)
30. M.C. Hiles, S.F. Badylak, G.C. Lantz, K. Kokini, L.A. Geddes, R.J. Morff, J. Biomed. Mater. Res. **29**, 883 (1995)
31. V. Mironov, G.D. Prestwich, G. Forgacs, J. Mater. Chem. **17**, 2054 (2007)
32. G.D. Prestwich, J. Cell. Biochem. **101**, 1370 (2007)
33. G.D. Prestwich, Y. Liu, B. Yu, X.Z. Shu, A. Scott, Adv. Enzyme Regul. **47**, 196 (2007)
34. X.Z. Shu, S. Ahmad, Y. Liu, G.D. Prestwich, J. Biomed. Mater. Res. **79**, 902 (2006)
35. Y. Liu, X.Z. Shu, G.D. Prestwich, Tissue Eng. **12**, 3405 (2006)
36. L. Flynn, G.D. Prestwich, J.L. Semple, K.A. Woodhouse, Biomaterials **28**, 3834 (2007)
37. R.A. Peattie, A.P. Nayate, M.A. Firpo, J. Shelby, R.J. Fisher, G.D. Prestwich, Biomaterials **25**, 2789 (2004)
38. R.A. Peattie, E.R. Rieke, E.M. Hewett, R.J. Fisher, X.Z. Shu, G.D. Prestwich, Biomaterials **27**, 1868 (2006)
39. D.B. Pike, S. Cai, K.R. Pomraning, M.A. Firpo, R.J. Fisher, X.Z. Shu, G.D. Prestwich, R.A. Peattie, Biomaterials **27**, 5242 (2006)
40. Y. Liu, S. Cai, X.Z. Shu, J. Shelby, G.D. Prestwich, Wound Repair Regen. **15**, 245 (2007)
41. M.S. Conte, R.P. Choudhury, M. Shirakowa, J.T. Fallon, L.K. Birinyi, R.P. Choudhry, J. Vasc. Surg. **21**, 413 (1995)
42. L.B. Kleinert, J.B. Hoying, S.K. Williams, Cell Transplant. **5**, 475 (1996)
43. M.C. Deruiter, R.E. Poelmann, J.C. Vanmunsteren, V. Mironov, R.R. Markwald, A.C. Gittenberger-De Groot, Circ. Res. **80**, 444 (1997)
44. Q. Shi, S. Rafii, M.H. Wu, E.S. Wijelath, C. Yu, A. Ishida, Y. Fujita, S. Kothari, R. Mohle, L.R. Sauvage, M.A. Moore, R.F. Storb, W.P. Hammond, Blood **92**, 362 (1998)
45. E.T. Yeh, S. Zhang, H.D. Wu, M. Korbling, J.T. Willerson, Z. Estrov, Circulation **108**, 2070 (2003)
46. Y. Liu, X.Z. Shu, G.D. Prestwich, Fertil. Steril. **87**, 940 (2007)
47. S. Cai, Y. Liu, X.Z. Shu, G.D. Prestwich, Biomaterials **26**, 6054 (2005)
48. K. Ghosh, X.D. Ren, X.Z. Shu, G.D. Prestwich, R.A. Clark, Tissue Eng. **12**, 601 (2006)
49. G.D. Prestwich, X.Z. Shu, Y. Liu, S. Cai, J.F. Walsh, C.W. Hughes, S. Ahmad, K.R. Kirker, B. Yu, R.R. Orlandi, A.H. Park, S.L. Thibeault, S. Duflo, M.E. Smith, Adv. Exp. Med. Biol. **585**, 125 (2006)
50. X.Z. Shu, K. Ghosh, Y. Liu, F.S. Palumbo, Y. Luo, R.A. Clark, G.D. Prestwich, J. Biomed. Mater. Res. **68**, 365 (2004)